Convective Heat Transfer Coefficients in a Building-Integrated Photovoltaic/Thermal System

Department of Building, Civil and Environmental Engineering, Concordia University
Room EV16.117, 1455 Maisonneuve W., Montréal, Québec, H3G 1M8
Tel. (514)-848-2424, ext. 7080, e-mail: lm_canda@encs.concordia.ca

Abstract

This paper presents an experimental study of interior convective heat transfer correlations for an open loop air-based Building Integrated Photovoltaic-Thermal system (BIPV/T) channel. The BIPV/T system absorbs solar energy on the top surface, which includes the photovoltaic panels and generates electricity while also heating air flowing in a channel between the top surface and an insulated attic layer. The BIPV/T system channel has a length/hydraulic diameter ratio of 38 which is representative for a BIPV/T roof system for 30-45-° tilt angle. The results show strong buoyancy effects (Rayleigh numbers in the range $2\times10^{10}<Ra<5\times10^{10}$) which enhance the heat transfer and that correspond to the mixed regime of convection heat transfer. Because of the heating asymmetry in the BIPV/T cavity, two Nusselt number correlations are reported: one for the top hot surface, and the other for the bottom surface. For the top heated surface the Nusselt number is in the range 6 to 48 for Reynolds numbers ranging from 250 to 7500.

1. Introduction

Building Integrated Photovoltaic/Thermal (BIPV/T) systems produce thermal and electrical energy while resulting in reduced effective costs when compared to stand alone PV systems [1] .The BIPV/T system absorbs solar energy on the top surface, which includes the photovoltaic panels and generates electricity while also heating air flowing in a channel between the top surface and an insulated attic layer. The PV modules replace cladding or roofing elements of the building envelope. Open loop air-based BIPV/T systems supply solar-heated air that can be used either for ventilation, direct space heating, heating through a heat exchanger or as a source for a heat pump [2, 3]. Accurate convective heat transfer coefficients (CHTCs) are essential for solving the energy balance equations used for lumped parameter network modelling of these systems (see Figure 1).

This is necessary to quantify its thermal and electrical energy production, which in turn provides adequate means for sizing associated equipment, such as heat exchangers and electrical inverters. The PV temperatures obtained by solving the energy balance equations for the PV module helps in designing the array layout and the electrical wiring in order to maximize electrical power production. These coefficients are also important for the development of control algorithms for control of the airflow [4].

So far researchers and engineers have relied on heat transfer correlations developed for similar geometries such as pipes and channels. This approach is not satisfactory due to the inherent complexity of BIPV/T channels, which include heating asymmetry, high aspect ratios, non-constant heat fluxes, non-uniform wall temperatures, non-developed flow conditions and non-uniform cross sections.

The focus of this work is the determination of the internal convective heat transfer coefficients for a BIPV/T system with outdoor air as the cooling fluid. The channel is smooth and has an aspect ratio width to height of 10. The channel studied is smooth in order to obtain the lower limits of the actual heat transfer coefficients.

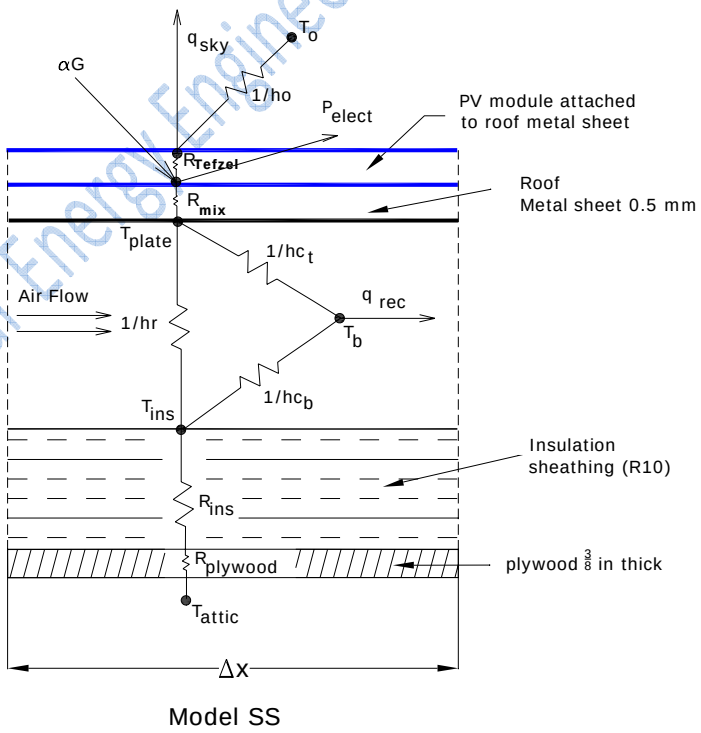

Fig. 1. Schematic representation of a BIPV/T thermal network model showing the interior convective heat transfer coefficients [1].

Figure 1 presents the energy fluxes in a typical BIPV/T system. T_o is employed to calculate the heat losses by convection heat transfer to the exterior. R_{Tefzel} and R_{mix} represent the thermal resistances by the PV module encapsulant, and the backing substrate and the metal sheet where is mounted. hc_t and hc_b represent the convective heat transfer coefficients from the top and bottom surfaces to the bulk air temperature (T_b). T_{plate} and T_{ins} represent the temperatures of the plate and the insulation used to compute the radiation heat transfer and the convective heat transfer coefficients. R_{ins} is the thermal resistance of the insulation.

1.1 Framing effects

PV modules are usually installed on the roof by means of custom made metallic or wood support structures, such as the one found in the BIPV/T system of the Northern Light Canadian Solar Decathlon 2005 house [5]. These structures enhance the heat transfer and change the local distribution of the convective heat transfer coefficients as studied in detail by CFD modeling [6]. Currently, experimental work is being carried out to quantify the effects on heat transfer and will be published in a follow up paper.

Fig. 2. Photo of the wood framing structure employed to support the PV modules in the Northern Light Canadian Solar Decathlon 2005 house [5].

2. Convective heat transfer coefficients

Numerous investigations report that typical correlations used to evaluate the heat transfer coefficient underestimate their actual values such as [7-10]. A short discussion of the literature available is presented below for BIPV/T applications and solar air heaters. A

discussion about mixed convection effects is presented as well. Some of the main correlations from the literature are summarized in Table 1.

2.1 Correlations employed in BIPV/T models

Eicker *et al.* [7] developed a model for a BIPV/T façade system and compared it to experimental data. It was reported that the model data could not fit the experimental results by using simple heat transfer correlations (e.g. parallel plate) to represent the heat transfer in the gap formed by the PV module and the colder glass. The reported heat transfer coefficients for an average air velocity of 0.3 m/s for a gap of 14 cm were 4 to 5 W/m^{2}K for the hot PV side. For the colder glass side the convective heat coefficient was 3 W/m^{2}K. Although the Reynolds number and Nusselt number were not reported, using the information provided the estimated Reynolds number is around 4800 and an estimated Nusselt number between 42 to 52 for the hot PV side and 31 for the colder glass side.

Bazilian *et al* [11] developed a numerical model for a photovoltaic heat recovery system. The model compared three different correlations, one for turbulent flow with uniform heat flux, another developed for smooth solar air collectors by Malik and Buelow [12] and the modified Petukhov equation or Gnielinski correlation [13, 14]. Bazilian and Prasad [8] presented another numerical model for a ventilated PV-roof façade for the natural convection case. A set of energy balance equations was written and solved. The authors point out that the model seemed to underestimate the outlet air temperature and overestimate the PV module temperature.

For solar air heaters, Eicker [15] recommends the use of the Petukhov equation for turbulent flow (Re>3100) and the Tan and Charters equation for fully developed turbulent flow [16]. For laminar flow Eicker recommends Nusselt number correlations by Altfeld [17] and Shah and London [18]. For vertical ventilated photovoltaic façades Eicker states that the free convection regime must be taken into account even when the flow is fan-driven. The recommendation is that the Nusselt number should be an average of the laminar and turbulent portion i.e. $Nu = \sqrt{{Nu_{lam}}^2 + {Nu_{turb}}^2}$.

Bloem [9] developed a numerical model in TRNSYS© for a PV façade. In the paper detailing the investigation it is stated that from measurements, the interior convective heat transfer coefficients were underestimated in the model.

Charron & Athienitis [10] used the Gnielinski correlation modified with the Hausen entrance factor [19] to estimate the heat transfer in a double facade. The authors conclude that the convective coefficient correlations were an underestimation of the actual heat transfer coefficients by about half. Another important conclusion is that the ratio of Gr/Re^2 has to be revised to determine if the flow is driven by natural, mixed, or forced convection.

Chen *et al.* [20] modeled a BIPV/T roof system with a correlation for turbulent flow [21].

Candanedo *et al.* [22] employed the Gnielinski correlation for turbulent flow and one for laminar developing heat transfer [23].

2.2 Correlations employed in Air hybrid photovoltaic/thermal (PV/T) collector models

Sopian *et al.* [24] employed a Nusselt number correlation for fully developed turbulent flow [13] for asymmetric heating to model a hybrid PV/T heater. Garg & Adhikari [25] employed the Tan and Charters correlation in their numerical model. Hegazy [26] used a Nusselt number correlation that contains an exponential correction to account for the diminishing convective heat transfer from the entrance [27].

Ong [28] employed different Nusselt number correlations depending on the fluid flow regime. For laminar flow he employed the Heaton correlation, for transitional the Hausen correlation, and for fully turbulent flow the Tan and Charters and the Petukhov correlations. The temperature error between predicted data with experimental was around 5 °C [28].

Ito *et al.* [29] used the Mercer correlation for laminar convection [13]. For forced convection he employed a modified version of the Kays and Crawford correlation which considers the developing flow conditions [13].

2.3 Context of the heat transfer correlations

The previous correlations are valid as long as the conditions for which they were developed are met. A brief description of how the correlations were obtained through

experiments is presented below which identifies under which conditions they would represent the convective heat transfer in a BIPV/T cavity.

Dittus & Boelter [30, 31] developed their equation for ducts by averaging the results of different researchers. Incropera and DeWitt [32] recommend the use of the Dittus and Boelter equation for Re>10,000 and length to D_h ratios (L/D) > 10. In contrast, McAdams [33], also recommends this equation but more restrictively. He recommends the use of this equation for the range 10,000<Re<120,000 and for ratios of L/D of 60 or more. McAdams [33] also recommends the equation for "moderate temperature differences" without giving detail on what can be considered moderate temperatures.
A correlation that has not been used in BIPV/T or in solar air collectors is the Martinelli equation [34]. This equation is recommended in Kakac & Yener [35] for turbulent flow in pipes and for parallel plates. The original paper contains typos in some of the equations. The corrected equations can be found in [33] and a list of the assumptions is given. One of the main features of the Martinelli equation is that it can explain the heat transfer behavior for different Prandtl numbers. It considers the use of the bulk air temperature to determine the heat transfer coefficient, and the friction factor.

Tan & Charters [36] studied the effect of the entrance length using a duct with 103 diameters of heated length. The Reynolds numbers ranged from 9500 to 22000. In the report there is no indication that the channel was tilted. The work was further expanded to present a Nusselt number for developed flows [16]. The experimental data showed lower heat transfer rates compared to Dittus and Boelter's equation. Results agree with those obtained by the Sparrow 's investigation for an asymmetrically heated channel [37]. In Sparrow's investigation, the duct had two sections, a first unheated one with a length of 40 Dh and the heated section with 140 Dh. It is important to mention that in Sparrow's investigation the orientation of the duct was horizontal. A clear description of the setup can be found in [38].
Cheng & Hong [39] did a numerical study with inclined tubes at low Reynolds number (5<Re<20). Strong buoyancy effects on heat transfer were found at Rayleigh numbers above 100 for the titled tube.

Experimental results from Malik & Buelow [40] were obtained using ducts of 162 D_h long. Although not explicitly stated, it appears that the duct was horizontal. Two ducts were analyzed, one with a flat cover and one with a corrugated cover.

2.4 Limitations of the Correlations that have been used in BIPV/T Modelling

Most of the correlations were done at high Reynolds numbers (above 10,000), and employed long heated lengths to find fully developed conditions. Also, most of the studies have been carried out in horizontal channels and pipes where buoyancy effects might not be as strong. In contrast, in a typical roof BIPV/T system, such as the one in EcoTerra Equilibrium demonstration solar house [3], the length of the system is 5.5m. It has an L/Dh ratio ≈ 70 and it is installed at a 30° tilt angle.

2.5 Mixed Convection Studies

Metais & Eckert [41] presented forced, mixed and free convection regime maps for flow through vertical and horizontal tubes. The objective of their investigation was to determine under which conditions forced or natural convection can be ignored. The authors acknowledged that "the limits between the various flow regimes have to be considered tentative until more experimental results are available".

Petukhov [42] presented equations to establish Grashof numbers when buoyancy effects will affect the heat transfer by 1% from its value for forced convection, for vertical pipes, and for horizontal pipes. The equations are functions of Reynolds and Prandtl numbers.

For vertical pipes

$$Gr_q = \frac{1.3\cdot10^{-4}Re^{2.75}Pr\left[Re^{1/8}+2.4\left(Pr^{2/3}-1\right)\right]}{\log(Re)+1.15log(5Pr+1)+0.5Pr-1.8} \quad (1)$$

For horizontal pipes

$$Gr_q = 3\cdot10^{-5}Re^{2.75}Pr^{0.5}\left[1+2.4\left(Pr^{2/3}-1\right)Re^{-1/8}\right] \quad (2)$$

Where, Gr_q

$$Gr_q = \frac{g\beta q_w D^4}{v^2 k} \quad (3)$$

Gnielinski [19] states that there are two main factors that influence the heat transfer coefficient for air, nitrogen, and helium: a) variable physical properties and b) natural

convection. Variable physical properties for gases do not increase the heat transfer more than 10%. However, the effect of free convection may increase the heat transfer three to four times more than the estimated heat transfer due to pure forced convection alone.

Jackson et al. [43] studied combined free and forced convection in a vertical tube where the temperature was constantly maintained. A Nusselt number correlation was developed.

Brown & Gauvin [44] studied combined free and forced convection in aiding flow in a vertical pipe. Aided or assisted flow occurs when air flows upward in a heated pipe and downward in a cooled pipe. Brown and Gauvin's results show a decrease in Nusselt numbers for laminar flow. However, for turbulent flow the heat transfer was augmented.

Axcell & Hall [45] carried out experiments for downward flow of air in a vertical pipe for Reynolds numbers between 20,000 to 130,000. For Reynolds number, 18,800 the measured Nusselt number was 164, which was more than 2.7 times higher than the Nusselt number predicted with the Petukhov and Kirillov equation and 3.1 times higher than the Nusselt number given by the Dittus-Boelter correlation. It was also compared against a correlation developed by Fewster & Jackson [46] for turbulent buoyant flows and still was 20 to 25% higher than what the equation was predicting.

Cebeci *et al.* [47] carried out a numerical study using the boundary layer equations applicable to a vertical duct. The objective of the investigation was to study the heat transfer behavior for assisted and opposed flows for different ratios of Gr/Re^2. The results show that for aided flow the Nusselt number increases. For opposed flows, when the ratios Gr/Re^2 are around 0.01 the Nusselt number increases as well.

A study on laminar mixed convection heat transfer for water flow in horizontal parallel plates with asymmetric heating was done by Osborne & Incropera [48]. It was found that the asymmetric heat flux caused higher Nusselt numbers at the bottom surface than at the top surface.

A comprehensive review on mixed convection in vertical tubes is presented by Jackson *et al.* [49]. In the paper it is stated, that for laminar mixed convection regimes in assisted flow convection in vertical tubes, the heat transfer is enhanced. It is important to point out however, that for some combinations of $Gr_b/Re^{2.7}$ in the turbulent flow mixed convection regime for pipes, the results show that there is heat transfer impairment. However in the opposite case of down flow, the heat transfer is always enhanced. The

same type of behavior is reported in the paper by Aicher & Martin [50]. The investigation was about mixed turbulent convection in vertical tubes.

Sudo *et al.* [51] carried out experiments in a vertical duct and explored the effect of aspect ratio on the heat transfer. Results were reported based on dimensional parameters. When $Gr_x/Re_x^{21/8}Pr^{1/2}$ is between 10^{-4} and 10^{-2}, in both aiding and opposing flow, the heat transfer is on average higher than those predicted by correlations. One of the figures shows the ratio of Nusselt number measured/Nusselt number predicted by the Dittus and Boelter correlation. Correlations are also presented based on aiding and opposing flows. In this investigation most of the time heat transfer enhancement for both assisting and opposing flows was found. More recently, Zhang & Dutta [52] studied mixed buoyancy assisted convection with asymmetric heating conditions in a vertical, square channel. The fluid employed was water. It was found that the Nusselt number was higher than predicted with the Gnielinski equation. The Nusselt numbers were also higher when compared to the Nusselt number ratio predicted by the Cotton and Jackson equation [49]. The authors presented a new equation in the work of Dutta *et al.* [53] to correlate Gr/Re with the Nusselt number ratio.

2.6 Friction factor correlation

Since many of the heat transfer correlations need a friction factor value in order to be evaluated, a friction factor equation had to be chosen. ASHRAE [54] recommends the use of the friction factor equation developed by Churchill [55]. The advantage of the equation is that it is valid for all ranges of Reynolds numbers (laminar, transitional and turbulent).

The equation is:

$$f = 8\left[\left(\frac{8}{Rey_{Dh}}\right)^{12} + \frac{1}{(A+B)^{1.5}}\right]^{1/12} \tag{4}$$

Where

$$A = \left[2.457ln\left(\frac{1}{\left(\frac{7}{Rey_{Dh}}\right)^{0.9} + \left(0.27\frac{\varepsilon}{Dh}\right)}\right)\right]^{16} \qquad B = \left[\frac{37530}{Rey}\right]^{16}$$

Table 1.
Nusselt number correlations for flow in a cavity or duct

Author / Reference	Correlation/ Comments	Flow & Heating conditions
Dittus-Boelter [30, 31, 56] [33]	$Nu = 0.023Re^{0.8}\mathrm{Pr}^{0.4}$	Average *Nu* for forced convection and symmetrical heating
	Recommended for fully developed turbulent (hydrodynamically and thermally) flow in pipes for Re≥10,000 and L/D≥10 0.7<Pr<160 [32] 10,000>Re>120,000 , L/D>60 and moderate ΔT[33]	
Gnielinski correlation [32]	$Nu = \frac{(Re - 1000)Pr\frac{f}{8}}{1 + 12.7\sqrt{\frac{f}{8}}(Pr^{\frac{2}{3}} - 1)}$	Average *Nu* for forced convection and symmetrical heating
	Smooth tubes, For 3000<Re<5×10^6 0.5<Pr<2000	
Modified Petukhov equation for and short channel length and [15] for pipes	$Nu = \frac{(Re - 1000)Pr\frac{f}{8}}{1 + 12.7\sqrt{\frac{f}{8}}(Pr^{\frac{2}{3}} - 1)}\left(1 + \left(\frac{D_h}{L}\right)^{2/3}\right)$	Average *Nu* for forced convection and symmetrical heating
	Where, $f = (0.79\ln(Re) - 1.64)^{-2}$ and Re≥3,000	
Tan and Charters [15] For air (Pr ≈ 0.71)	$Nu = 0.0158Re^{0.8} + (0.00181Re + 2.92)e^{(-0.03795L_c/D_h)}$	Average *Nu* for forced convection and asymmetrical heating
	for a horizontal duct, Re>9500	
Martinelli [33] Note: Original Nu correlation presented in [34] but had typographical errors and was corrected in	$Nu = \frac{Re \cdot Pr \cdot \sqrt{f/2}}{\left(\frac{tw - tb}{tw - tc}\right) \cdot 5 \cdot \left(Pr + ln(1 + 5Pr) + 0.5N_{DR}ln\left(\frac{Re}{60}\sqrt{\frac{f}{2}}\right)\right)}$	Average *Nu* for forced convection and symmetrical heating

[33].	Where T_w is the temperature of the wall, T_b the bulk air temperature, and T_c temperature at the center of the pipe. NDR is plotted against Re and Pr in [34], for air Pr=0.71 and 1000<Re<10000, 0.7<N_{DR}<0.98. tw-tb = Δtmean, tw-tc = Δtmax For air (Tw-Tb)/(tw-tc) 0.78 to 0.84 for 2000<Re< 10000	
Malik and Bluelow [11]	$$Nu = \frac{0.0192Re^{\frac{3}{4}}Pr}{1 + 1.22Rey^{-\frac{1}{8}}(Pr - 2)}$$	Average *Nu* for forced convection and asymmetrical heating
	Recommended for 10000<Re<40000 and L/D_h>162	
Mercer correlation [13]	$$Nu = 4.9 + \frac{0.0606\left(\frac{RePrDh}{L}\right)^{1.2}}{1 + 0.0909\left(RePr\frac{Dh}{L}\right)^{0.7}Pr^{0.17}}$$	Average *Nu* for forced laminar convection and asymmetric heating
	Laminar flow Re<2300	

3. Experimental Setup

The experimental test rigs used in this research consist of a near full-scale BIPV/T system and a solar air heater in an outdoor test facility. The BIPV/T system can be considered a small scale version of the roof BIPV/T system in the EcoTerra Equilibrium demonstration solar house, See Figure 3 [3].

The experiments were carried out outdoors. Clear sky days with low wind conditions were chosen so as to be able to determine the exterior heat loss coefficient ho with sufficient accuracy.

Fig. 3. Photo of the BIPV/T roof in the EcoTerra House. The amorphous PV modules are attached to vertical and horizontal wood framing that also creates the flow channel. The roof has a length of 5.5 m.

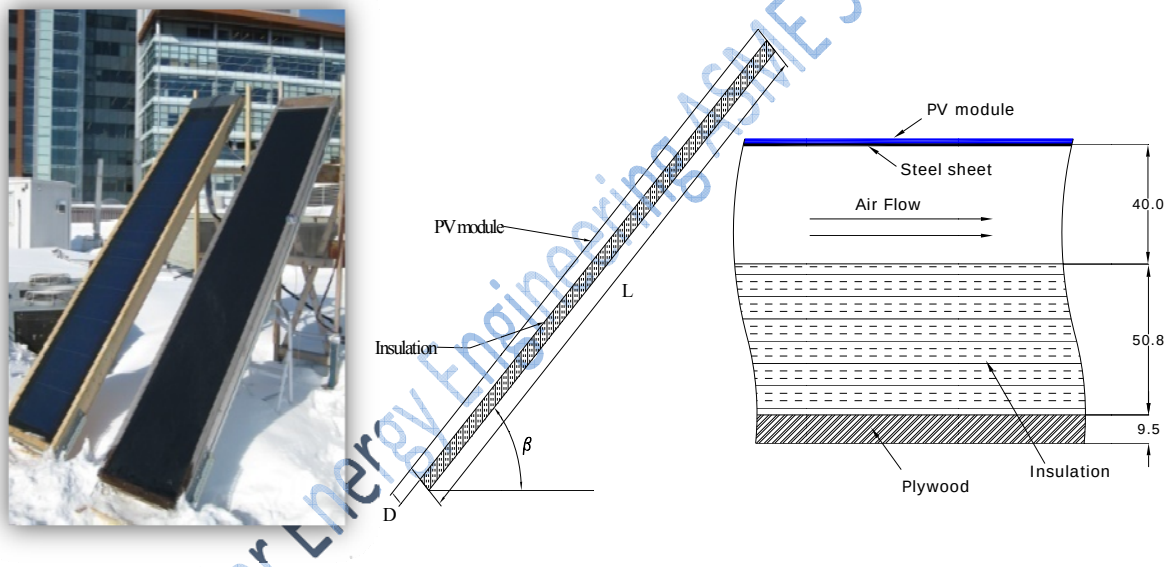

Fig. 4. From left to right (a) experimental BIPV/T setup replicating 1 strip of the BIPV/T of the EcoTerra house. (b) cross section of the setup. (c) close up of the cross section. The channel without the PV module is employed to determine the effect of attaching PV panels on heat generation [1].

The BIPV/T channel employs an amorphous PV module with an electrical efficiency of 6% at standard test conditions. This module was attached through built-in adhesive to a steel metal roof sheet with a thickness of 0.5 mm. The cross sectional area of the channel A_c was 0.01549 m^2. The hydraulic diameter D_h is given by $4A_c/U$, where U is the wetted perimeter(D_h= 0.074 m). The length of the channel was 2.84 m. The thermocouples were special limit T-type with a 0.3 °C maximum error. The tilt angle of the channel was 45°.

The channel is smooth and has no framing. The bottom of the channel consists of 2 inches of polysterene insulation R-10 (1.76 Km^2/W) and 3/8 in. thick plywood board (see Figure 4).

Since the major thermal gradients happen along the direction of the flow, 40 thermocouples were placed in the middle of the channel from the inlet to the outlet. Infrared photos of the metal channel showed insignificant thermal variation along the width. The same type of behavior was reported by Ong [28]. The following temperatures were measured: average inlet and outlet air temperature, the temperature of the interior side of the metal plate and the surface temperature of the insulation.

The electrical energy production was recorded every minute by a data acquisition system. The PV module was connected to a charge controller with a maximum power point algorithm. The wind speed and ambient air temperature were being recorded by a weather station. The anemometer was a 3-cup type. The wind speed and the ambient air temperature sensors were placed about 10 m above ground.

The convective heat transfer in the cavity was calculated using the equation:

$$Qc_{in} = \dot{m} \cdot c_p \cdot (T_{out} - T_{inlet}) \quad (5)$$

T_{out} is the average temperature of the air at the outlet and T_{inlet} is the average air temperature at the inlet. The specific heat cp is given by the equation:

$$c_p = c_{pa} + W \cdot c_{pv} \quad (6)$$

where W is the air moisture content, cpa is the specific heat of dry air and has the value of 1.0 $kJ/(kg_a\text{-}K)$ and c_{pv} 1.86 $kJ/(kg_v\text{-}K)$.

The moisture content of the air has been calculated using the relative humidity (RH) and the dry bulb temperature. The saturation pressure has been calculated with the formulas provided by ASHRAE [54].

The mass flow rate was measured using a laminar flow element (LFE). The LFE comes with a calibration curve in order to determine the "Actual Volumetric Flow Rate". This curve is given as a function of the pressure drop measured across the LFE and the inlet temperature of the fluid. The curves have the form:

$$ACFM = \left(A + B\Delta P + C\Delta P^2 + D\Delta P^3\right) \cdot \frac{181.8718}{\mu_f} \cdot T_{cf} \quad (7)$$

where ACFM stands for the actual volumetric flow in CFM. A, B, C and D are calibration constants for each instrument, T_{cf} is a temperature correction factor, given by $T_{cf} = 529.67/(459.67+^{\circ}F)$ and the viscosity of the fluid is given by:

$$\mu_f = \left(\frac{14.58\left(\frac{459.67 + °F}{1.8}\right)^{3/2}}{(110.4 + \left(\frac{459.67 + °F}{1.8}\right)} \right) \quad (8)$$

Where °F is the average air temperature of the fluid in Fahrenheit degrees. Equation (8) has the same form as Sutherland's approximation for the viscosity of gases [57].

When performing the measurement it is advisable to take a time-averaged reading for the pressure differential. It was found that taking 40 measurements per minute gave a reading that was sufficiently representative for the flow rate calculations. The LFE was calibrated for a range of 0 to 105 CFM. The pressure drop at the maximum flow rate was about 8 inches of water. For this LFE the largest error was 0.37% of the full scale (FS). The fan can provide up to 48 CFM through the channel. The pressure transducer used for the LFE (also Setra 267) can measure pressure from 0 to 10 inches of water with 0.25% FS accuracy.

The radiation exchange between the interior surface of the metal plate and the insulation surface is given by

$$Q_{radin} = \frac{F_{pv} \cdot Area \cdot \sigma \cdot (T_{plate}^{\ 4} - T_{insu}^{\ 4})}{\frac{1}{\varepsilon_1} + \frac{1}{\varepsilon_2} - 1} \quad (9)$$

where ε_1 and ε_2 correspond to the emissivities of the surfaces. The measured emissivity of the steel plate was 0.80 while the corresponding value for the insulation board was 0.20. $F_{pv,b}$ is the view factor between the two cavity surfaces [32]

3. 1 Time Response

The air BIPV/T channel would usually reach steady state temperature distribution after 8 or 9 minutes for quasi constant solar radiation and exterior wind speed as shown in Figure 5.

Kakac [58] studied the effect of step changes in the boundaries of a channel with a numerical analysis. The analysis for Re 9370 would need an approximate time of 0.07 seconds to reach steady state for the dimensions of the channel. This analysis however does not consider the capacitance and resistance of the materials.

A practical way of analyzing the time response of the system is to consider it a simple RC circuit, or a lumped thermal capacitance model. The time required to fall *by 63%* is the product of RC. A recommended time to reach steady state is to use five times the value of RC. The combined thermal capacitance of the module and the steel sheet was 7838 J/m^2K, with a combined thermal resistance of 0.011 m^2K/W. The time constant, (RC), was 86.2 seconds. In order to reach a steady state condition we can multiply the time constant times 5, then 5*86.2= 431 s or 7.2 minutes. This value is significantly close to the value cited above (8-9 minutes).

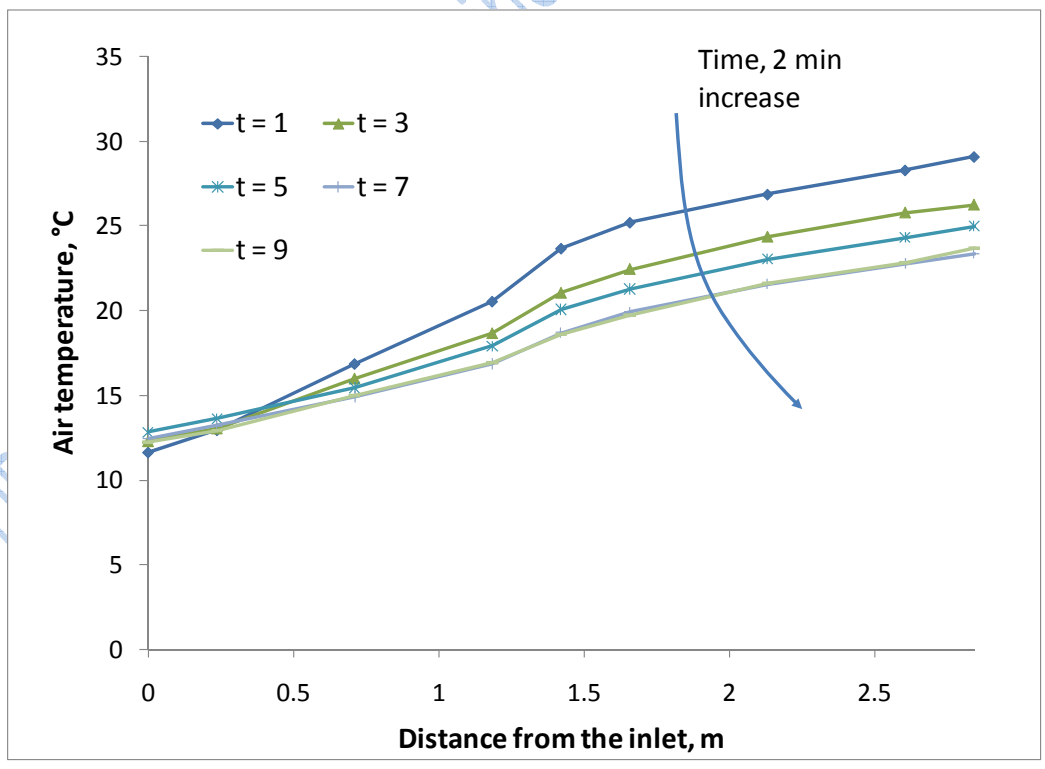

Fig. 5. Time response of the bulk air temperature for constant flow rate and solar radiation.

The bulk air temperature rise in the channel follows an exponential trend. In order to eliminate local irregularities on the final results, the experimental data was fitted using an exponential equation with Mathcad [59]. The fitting is based on an optimized version of the Levenberg-Marquardt method for minimization.

The equation has the following form

$$T_{bulkair}(x) = A\left(1 - e^{-\frac{x}{B}}\right) + C \quad (10)$$

where A, B, and C are fitted parameters. The correlation coefficients (R^2) of the regressions shown in Figure 6 are high ($R^2 \approx 0.99$).

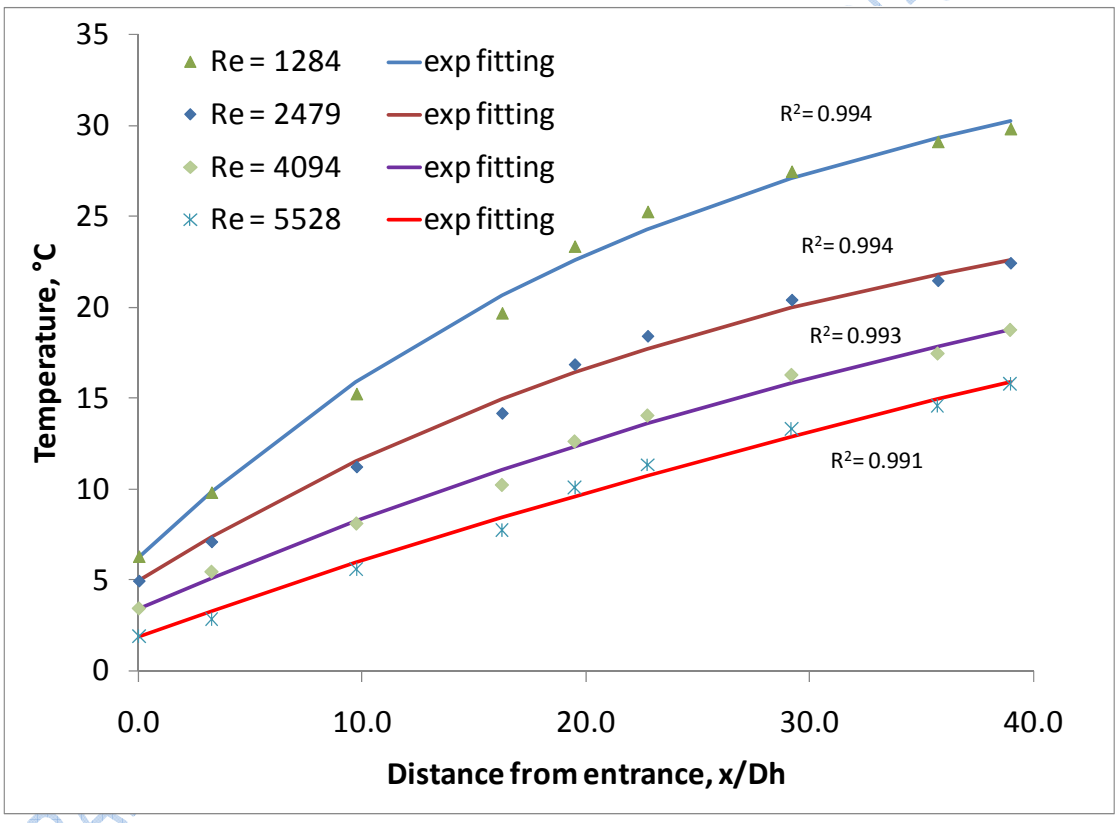

Fig. 6. Air bulk temperature for different Reynolds number compared with exponential fitting.

3.2 Computation of Convective Heat Transfer Coefficients

In order to compute the average internal instantaneous CHTC it was necessary to obtain the averaged temperatures of the PV and the insulation (T_{PV} and T_{ins}) each minute. Since the air temperature increase is expressed by the exponential formula, local coefficients

can be calculated for different control volumes. Then the convective heat transfer coefficient for the top plate was computed as

$$\mathrm{hc_{top}} = \frac{\mathrm{Qincv} - \mathrm{Qradincv}}{\mathrm{A_{cv}}\left(\overline{\mathrm{T_{plate}}} - \overline{\mathrm{T_b}}\right)} \tag{11}$$

where Q_{incv} is found with equation 5 and $Q_{rad\_in\ plates}$ was computed with equation 9.

For the bottom surface,

$$hc_{bot} = \frac{\mathrm{Qradincv}}{\mathrm{Acv}\left(\overline{\mathrm{T}}_{\mathrm{instcv}} - (\overline{\mathrm{T}}_{\mathrm{b}})\right)} \tag{12}$$

In this analysis, the bottom heat loss can be considered negligible due to the high value of the insulation.

Two Nusselt numbers, one for each of the boundaries have been used before in parallel plates, channels by [60] [37] [48] and for asymmetric heating in concentric circular tubes [61].

The Nusselt numbers are in turn given by

$$\mathrm{Nu_{top}} = \frac{\mathrm{hc_{top}} D_h}{\mathrm{k_{air}}} \tag{13}$$

For the top

$$\mathrm{Nu_{bot}} = \frac{\mathrm{hc_{bot}} D_h}{\mathrm{k_{air}}} \tag{14}$$

For the bottom surface

4. Results and Discussion

4.1 Local effects

The local Nusselt numbers are plotted in Figure 7. As can be seen when the flow is turbulent, it reaches fully developed conditions in shorter lengths. The behavior is opposite for the laminar flow conditions.

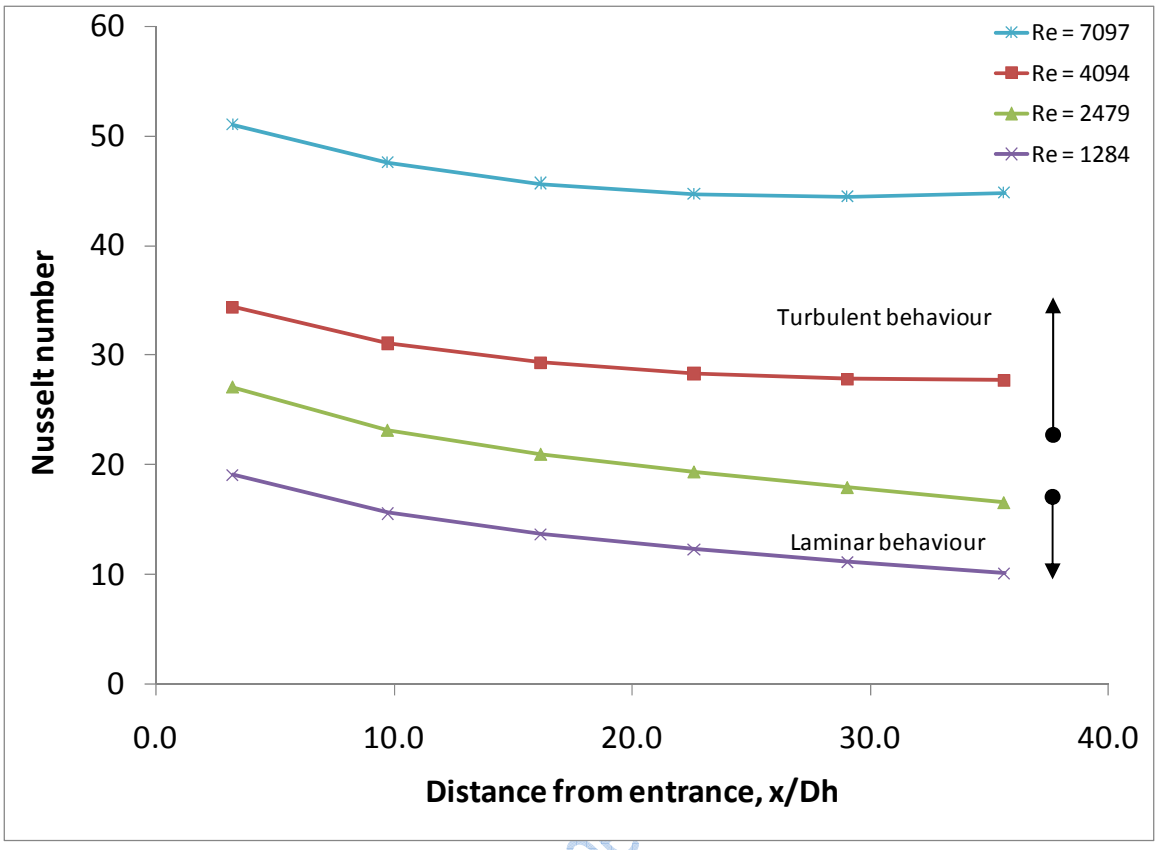

Fig. 7. Local Nusselt number for the top surface versus non dimensional distance from the entrance.

Kays [61] recommends for the entry length solution for the circular tube the relationship

$$\frac{x}{D} \approx 0.05RePr \quad (15)$$

While Hallman [62] employs the relationship

$$\frac{x}{D} > 0.0425RePr \quad (16)$$

To obtain the fully develop solution for the laminar flow (Re<2300).

However for the turbulent region, White [63] states that the developing length is shorter and it can be calculated with

$$\frac{x}{D} \approx 4.4Re^{1/6} \quad (17)$$

The experimental results agree with the previous formulas to determine the developing length. For instance at Reynolds ≈ 1284, x/D ≧ 38.7 after using equation 16. For Re ≈ 4094, x/D ≧ 17.6 (equation 17).

4.2 Average Nusselt Numbers

The average Nusselt number coefficients for the top and the bottom surfaces are calculated from the local distributions and plotted as a function of the Reynolds number. A correlation for the Nusselt and the Reynolds number has been obtained. It was found by means of an optimized version of the Levenberg-Marquardt method for minimization [59].

For the top surface

$$Nu_{top} = 0.052Re^{0.78}Pr^{0.4} \quad (18)$$

And for the bottom surface

$$Nu_{bottom} = 1.017Re^{0.471}Pr^{0.4} \quad (19)$$

The correlations along with the uncertainty in the data are plotted in Figures 8 and 9. As can be seen, the Nusselt numbers for the bottom surface are higher than the ones from the top surface. Sparrow *et al.* [37] found the same behavior in the experimental results where the heated wall has a lower Nusselt number than the unheated one. In our case, because the bottom surface is insulated, the heat gain by longwave radiation from the top heated surface is approximately equal to the heat transfer to the air by convection, thus resulting in a small temperature differential between the bottom surface and the air.

The uncertainties for the top surface are very small. They range between 4.3% to a maximum of 7% at low Reynolds numbers. The highest uncertainties occur at the lowest Reynolds numbers. The same behavior has been reported by Novotny *et al* [38].

The experimental results show significantly more uncertainty regarding the heat transfer coefficients of the bottom surface; however, their effect is far less important than that of the heat transfer coefficients of the top heated surface.

The high uncertainties are due to the fact that the air bulk temperature and the surface temperature are very close so that small error in the temperature measurement can cause high errors. Barrow [64] obtained scattered results in the data because of high uncertainty.

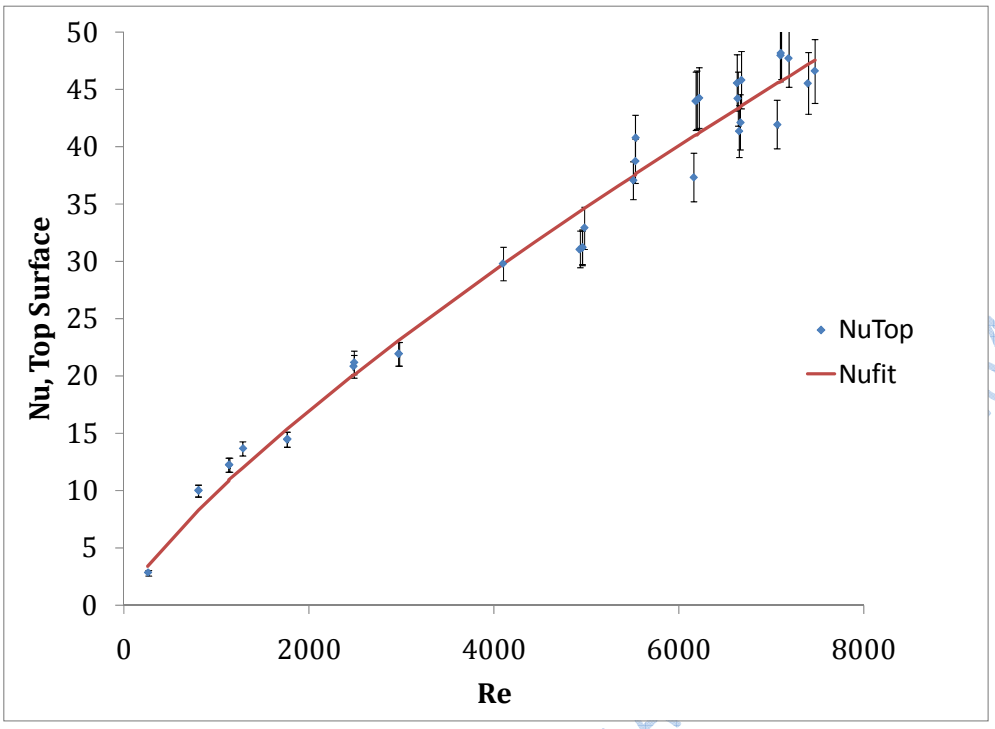

Fig. 8. Nusselt numbers for the top surface versus Reynolds number. The data is compared with the correlation given by equation 18. The uncertainties of each of the data points are plotted as well.

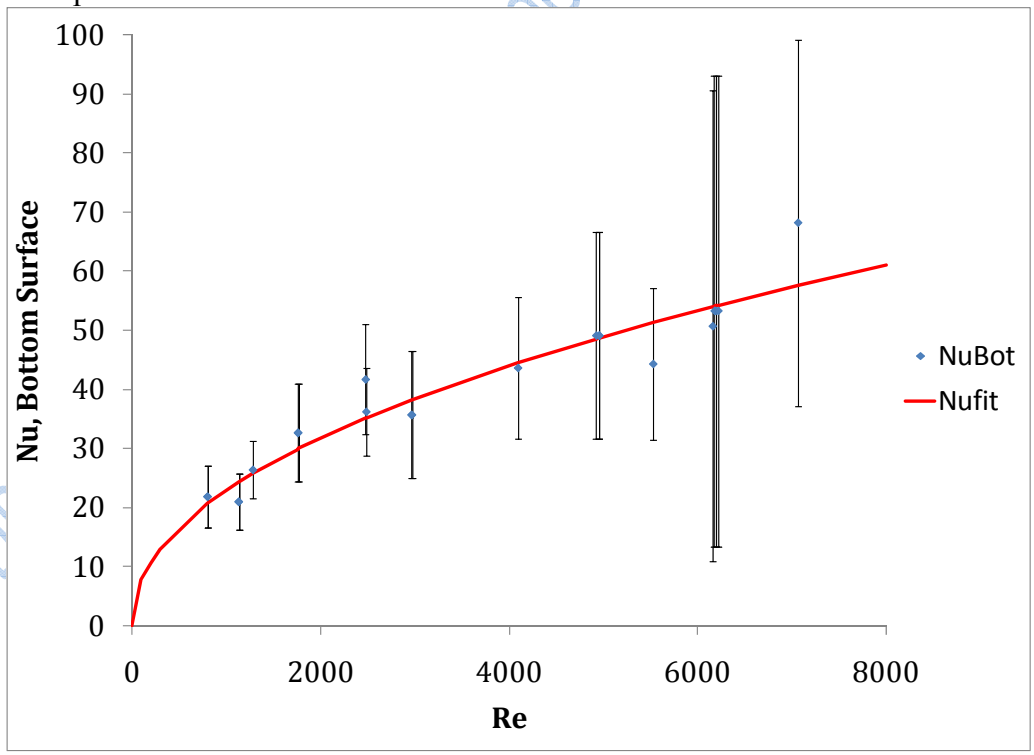

Fig. 9. Nusselt numbers for the bottom surface versus Reynolds number. The data is compared with the correlation equation 19. The uncertainties of each of the data points are plotted as well.

4.3 Comparison of the new correlation with previous results

The Nusselt numbers for the top surface are compared with a few of the most typical correlations in Figure 10. The equations were evaluated with the friction coefficient proposed by Churchill [55].

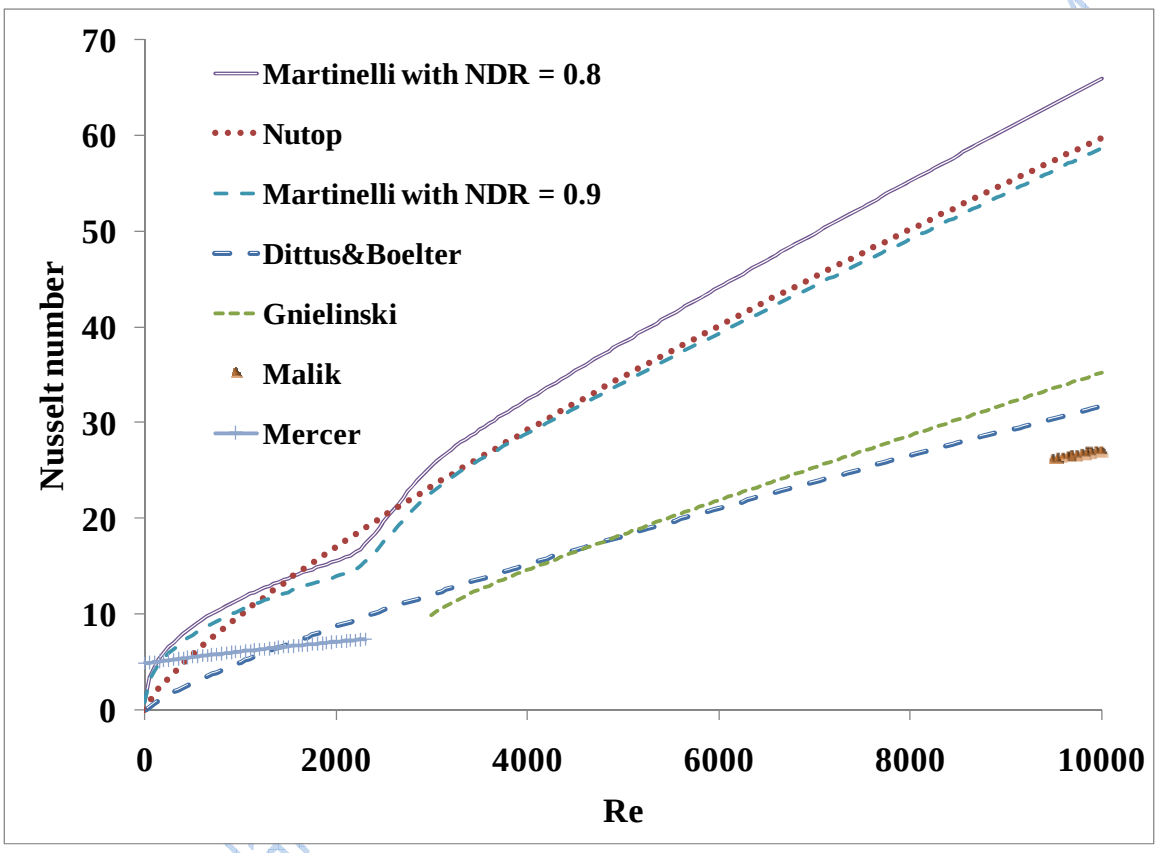

Fig. 10. Comparison of the top Nusselt number correlation with Dittus-Boelter, Gnielinski, Martinelli, Malik and Mercer correlations.

Although Dittus-Boelter's equation is recommended, for Re> 10,000, it has been plotted to indicate the possible low limit of the heat transfer. As can be seen from Figure 10 the Dittus-Boelter and Gnielinski equations predict very similar values. Martinelli's equation includes a correction for the ratio of temperature difference of the wall and the bulk air temperature. Martinelli's equation predicts the measured Nusselt number for the top surface very close to the current correlation. The experiment, in general, shows higher

values of Nusselt numbers in the low Reynolds number compared to the Mercer correlation and is mainly due to the fact that fully developed conditions are not attained.

4.4 Grashof and Rayleigh numbers of experimental data

Petukhov [42] pointed out that when Grashof numbers surpass a certain upper limit, actual Nusselt numbers will be at least 1% higher than the value predicted by forced convection correlations for circular pipes. This "maximum" Grashof number is a function of the Reynolds number (Figure 11), and is different for vertical and horizontal pipes. As can be seen in Figure 11, the Grashof numbers experimentally measured in the BIPV/T channel exceed, by several orders of magnitude, Petukhov's upper limit curves. This indicates that forced convection correlations commonly used for circular pipes will be inadequate for the cases discussed in this paper, in which natural convection effects will clearly play a major role.

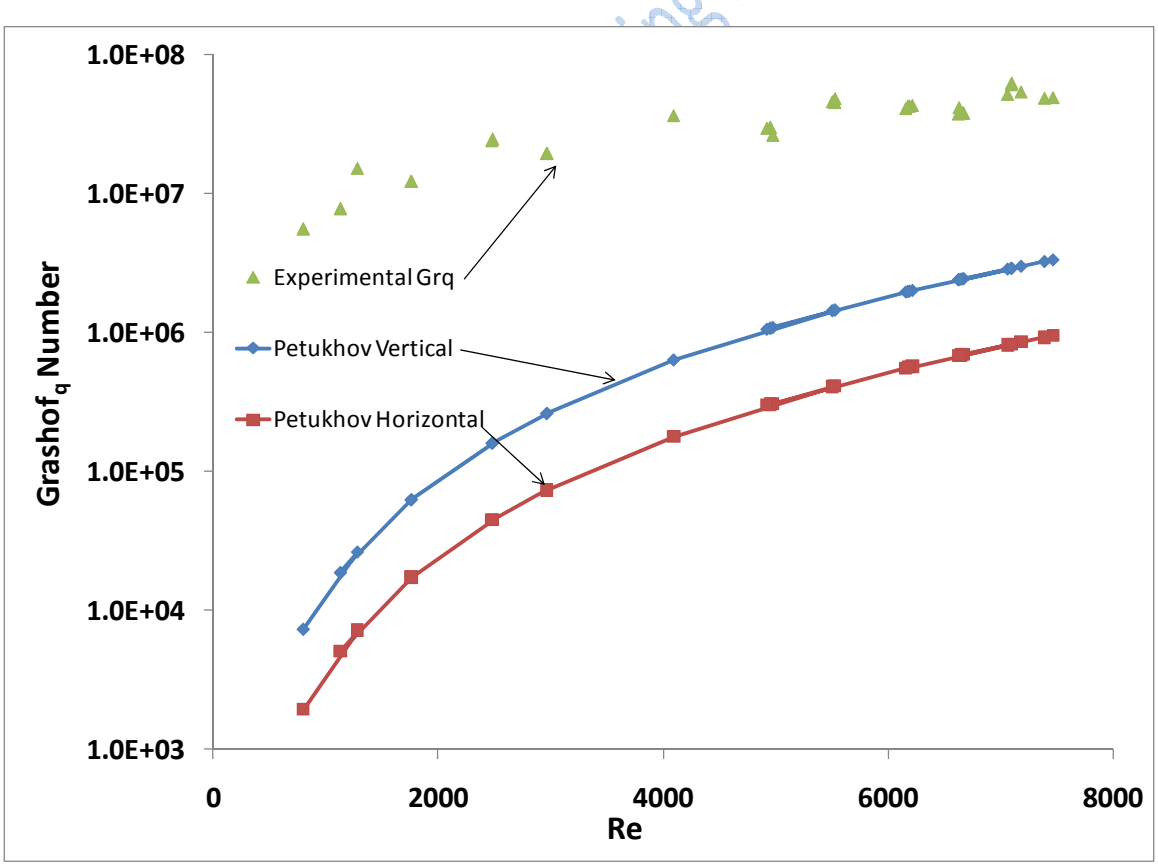

Fig. 11. Comparison of Equation 1 and 2 with the experimental data (Pr=0.71). All the experimental points are above the limits established by the equations.

The experimental data can be compared to the Metais & Eckert maps [41]. Most of the experimental data falls in the mixed regime of turbulent heat transfer ($2\times10^{10}<Ra<5\times10^{10}$). The experimental data is also in agreement with the results obtained by Sudo *et al.* [51] in a vertical heated rectangular channel, for which the Nusselt number is 1.7 to 2.4 times the value of the Dittus-Boelter equation.

5. Conclusion

Experimental measurements of the convective heat transfer coefficients have been carried out for a BIPV/T system. The coefficients are significantly higher than the values predicted by the forced convection equation given by Dittus and Boelter, Gnielinski, and Petukhov [31, 32] .Many of the studies were done for very long and horizontal channels, and high Reynolds numbers, where buoyancy effects are minimal.

The resulting higher Nusselt numbers are not surprising since the strong natural convection effects increase the heat transfer. The data also confirms evidence found by other researchers [7-10] that the Nusselt numbers were underestimated. The Martinelli equation proved to have the best agreement with the present experimental data. This is due to the fact that the equation takes into account the temperature difference between the wall and the bulk air temperature.

Correlations 18 and 19 are suggested for the determination of the Nusselt number for BIPV/T systems and solar air heaters for tilt angles around 45º.

Acknowledgements

This work was funded by the Canadian Solar Buildings Research Network, a strategic NSERC research network and NRCan-CanmetENERGY (Varennes). The technical assistance of Joseph Hrib and Kwang Wook Park in the set up of the experiment is gratefully acknowledged.

Nomenclature

G = total incident solar radiation, W/m^2
α = solar absorptivity,
A = collector exposed area, m^2
A_c = cross sectional area, m^2
U = wetted perimeter, m
h_c = convective heat transfer coefficient in cavity, $W/m^2 \cdot K$
k = thermal conductivity, $W/m \cdot K$
h_o, h_w = exterior convective heat transfer coefficient or wind coefficient, $W/m^2 \cdot K$
h_{ro} = exterior radiative heat transfer coefficient, $W/m^2 \cdot K$
h_r = cavity radiative heat transfer coefficient, $W/m^2 \cdot K$
C_{pv} = Thermal capacitance per unit area, $J/(K \cdot m^2)$
C_p = specific heat capacity of the air, $J/kg \cdot K$
Gr_q = Grashof number based on heat flux q_w, $(g\beta q_w D_h{}^4)/(\upsilon^2 k)$
q_w = heat flux on the wall, W/m^2
Gr = Grashof number, $g\ \beta(T_w - T_{bulk})D_h{}^3/\upsilon^2$
f = Friction factor
ρ = air density, kg/m^3
m = average mass flow rate, kg/s
D_h = hydraulic diameter of the cavity, m
Re = Reynolds number, $\rho V D_h/\mu$
Ra = Rayleigh number, $GrPr = g\rho^2 c_p\ \beta(T_w - T_{bulk})D_h{}^3/(\mu k) = g\ \beta(T_w - T_{bulk})D_h{}^3/\upsilon\alpha$
μ = dynamic or absolute viscosity, $kg/(m \cdot s)$
υ = kinematic viscosity, μ/ρ, m^2/s
g = gravitational acceleration, m/s^2
N_u = Nusselt number, hD_h/k
T_o, T_a = exterior air temperature, °C
T_{plate} = interior side temperature of the metal sheet, °C
T_{ins} = interior side temperature of the insulation, °C
T_{dp} = dew Point temperature, °C
T_{bulk} = air bulk temperature in the control volume, °C
T_{sky} = sky temperature, K
L = length of the channel, m
β = Thermal expansion Coefficient, 1/T
θ = tilt angle, degrees
V = average air velocity in the channel, m/s
V_w = average wind velocity, m/s
E_p = electric power, W
R_{ins} = insulation R value, m^2K/W
Q = heat transfer rate, W
η_e = electrical efficiency
Pr = Prandlt number, ν/α

α	= thermal diffusivity, $k/\rho c_p$
σ	= Stefan Boltzmann constant, W/m^2K^4

Acronyms

BIPV/T	Building Integrated Photovoltaic/Thermal
CHTC	convective heat transfer coefficient
CFM	Cubic feet per minute, ft^3/min
FS	Full span

References

[1] Candanedo, L.M., A.K. Athienitis, J. Candanedo, W. O'Brien, and Y.-X. Chen, *Transient and steady state models for open-loop air-based BIPV/T systems.* ASHRAE transactions, 2010.

[2] Candanedo, J. and A.K. Athienitis. *Simulation of the performance of a BIPV/T system coupled to a heat pump in a residential heating application.* in *9th International IEA Heat Pump Conference*. 2008. Zurich, Switzerland.

[3] Chen, Y., A.K. Athienitis, K.E. Galal, and Y. Poissant. *Design and Simulation for a Solar House with Building Integrated Photovoltaic-Thermal System and Thermal Storage*. in *ISES Solar World Congress, Beijing, China*. 2007.

[4] Candanedo, J.A., *Investigation of anticipatory control strategies in a net-zero energy solar house.* ASHRAE transactions, 2010.

[5] Pasini, M. and A.K. Athienitis, *Systems Design of the Canadian Solar Decathlon House.* ASHRAE Transactions 2006. **112, part 2**.

[6] Candanedo, L.M., W. Obrien, and A.K. Athienitis. *Development of an air-based open loop building-integrated photovoltaic/thermal system model*. in *Building Simulation 2009*. 2009. University of Strathclyde, Glasgow.

[7] Eicker, U., V. Fux, D. Infield, L. Mei, and K. Vollmer. *Thermal Performance of building integrated ventilated PV facades*. in *Proceedings of International Solar Energy Conference, Jerusalem* 1999.

[8] Bazilian, M.D. and D. Prasad, *Modelling of a photovoltaic heat recovery system and its role in a design decision support tool for building professionals.* Renewable Energy 27, 2002: p. 57-68.

[9] Bloem, J.J., *A TRNSYS type calculation model for double skin photovoltaic facades.* Proc. 19th European Photovoltaic Solar Energy Conference and Exhibition, Paris, France, 2004, 2004.

[10] Charron, R. and A.K. Athienitis, *A two dimensional model of a double facade with integrated photovoltaic panels.* Journal of Solar Energy Engineering, ASME, 2006. **128**: p. 160-167.

[11] Bazilian, M., N.K. Groenhout, and D. Prasad. *Simplified numerical modelling and simulation of a photovoltaic heat recovery system*. in *17th European photovoltaic solar energy conference*. 2001. Munich, Germany.

[12] Cengel, Y., *Heat Transfer: A practical approach*, ed. McGraw-Hill. 1998, New York.

[13] Duffie, J.A. and W.A. Beckman, *Solar engineering of thermal processes*. Third ed. 2006, Hoboken: John Willey & Sons, Inc. 908.

[14] Kakac, S., R.K. Shah, and W. Aung, *Handbook of single-phase convective heat transfer*. 1st ed, ed. J.W. Sons. 1987.
[15] Eicker, U., *Solar technologies for buildings*. First ed, ed. J. Wiley. 2003, West Sussex.
[16] Tan, H.M. and W.W.S. Charters, *An experimental investigation of forced convective heat transfer for fully developed turbulent flow in a rectangular duct with asymetric heating.* Solar Energy, 1970.
[17] Altfeld, K., *Exergetische Optimierung flacher solarer Lufterhitzer*, ed. V. Verlag. 1985: VDI Verlag.
[18] Shah, R.K. and A.L. London, *Laminar flow forced convection in ducts*. 1st ed. Advances in Heat Transfer, ed. J.a.J.P.H. Thomas F. Irvine. 1978, New York: Academic Press. 477.
[19] Gnielinski, V., *Forced convection in ducts*. Heat exchanger design handbook. , ed. U. Schlunder. Vol. 2. 1983, New York: Hemisphere Publishing Corporation.
[20] Chen, Y., A.K. Athienitis, B. Berneche, and P. Y. *Design and simulation of a building integrated photovoltaic thermal system and thermal storage for a solar home.* in *2nd Canadian Solar Buildings Conference*. 2007. Calgary.
[21] Kreith, F. and M.B. Bohn, *Principles of Heat Transfer*. 6th ed, ed. Brooks/Cole. 2001, Pacific Grove, CA.
[22] Candanedo, J.A., S. Pogharian, A.K. Athienitis, and A. Fry, *Design and simulation of a net zero energy healthy home in Montreal.* 2nd Canadian Solar Buildings Conference, 2007. **1**: p. 1-8.
[23] Lienhard, J.H.I. and J.H.V. Lienhard, *A heat transfer textbook*. 3rd ed. 2008, Cambridge, MA: Phlogiston Press.
[24] Sopian, K., K.S. Yigit, H.T. Liu, S. Kakac, and T.N. Veziroglu, *Performance Analysis of photovoltaic thermal air heaters.* Energy Conversion and Management, 1996. **37**(11): p. 1657-1670.
[25] Garg, H.P. and R.S. Adhikari, *Conventional hybrid photovoltaic/thermal (PV/T) air heating collectors: steady-state simulation.* Renewable Energy, 1997. **11**(3): p. 363-385.
[26] Hegazy, A.A., *Comparative study of the performance of four photovoltaic/thermal solar air collectors.* Energy Conversion & Management, 2000. **41**: p. 861-881.
[27] Altfeld, K., W. Leiner, and M. Fiebig, *Second Law optimization of flat plate solar air heaters. Part 1: the concept of net exergy flow and the modeling of solar air heaters.* Solar Energy, 1988. **41**(2): p. 127-32.
[28] Ong, K.S., *Thermal performance of solar air heaters experimental correlation.* Solar Energy, 1995. **55**: p. 209-220.
[29] Ito, S., M. Kashima, and N. Miura, *Flow control and unsteady-state analysis on thermal performance of solar air collectors.* Journal of Solar Energy Engineering, ASME, 2006. **128**: p. 354-359.
[30] Dittus, F.W. and L.M.K. Boelter, *Heat transfer in automobile radiators of the tubular type.* International Communications in Heat and Mass Transfer, 1985. **12**(1): p. 3-22.
[31] Dittus, F.W. and L.M.K. Boelter, *Heat transfer in automobile radiators of the tubular type.* University of California Publications, 1930. **2**(13): p. 443-461.

[32] Incropera, F.P. and D.P. De Witt, *Fundamentals of heat and mass transfer*. Fifth ed. 2002: John Wiley & Sons. 981.
[33] McAdams, W.H., *Heat Transmission*. 3rd ed. Series in Chemical Engineering, ed. McGraw-Hill. 1954: McGraw-Hill. 532.
[34] Martinelli, R.C., *Heat transfer to Molten Metals.* Transactions ASME, 1947. **69**: p. 947-959.
[35] Kakac, S. and Y. Yener, *Convective Heat Transfer*. 2nd ed. Vol. 1. 1995, Boca Raton, Florida: CRC Press. 422.
[36] Tan, H.M. and W.W.S. Charters, *Effect of thermal entrance region on turbulent forced convective heat transfer for an asymmetrically heated rectangular duct with uniform heat flux.* Solar Energy, 1969. **12**: p. 513-516.
[37] Sparrow, E.M., J.R. Lloyd, and C.W. Hixon, *Experiments on Turbulent heat transfer in an asymmetrically heated rectangular duct.* Journal of Heat Transfer. Transactions of the ASME., 1966. **88**: p. 170-174.
[38] Novotny, J.L., S.T. McComas, E.M. Sparrow, and E.R.G. Eckert, *Heat transfer for turbulent flow in rectangular ducts with two heated and two unheated walls.* A.I.Ch.E. journal, 1964. **10**(44): p. 466-470.
[39] Cheng, K.C. and S.W. Hong, *Effect of tube inclination on laminar convection in uniformly heated tubes for flat-plate solar collectors.* Solar Energy, 1972. **13**: p. 363-371.
[40] Malik, M.A.S. and F.H. Buelow. *Heat transfer characteristics of a solar drier*. in *Sun Service Mankind*. 1973. Paris.
[41] Metais, B. and E.R.G. Eckert, *Forced, mixed and free convection regimes.* Journal of Heat Transfer, 1964: p. 295-296.
[42] Petukhov, B.S., *Turbulent flow and heat transfer in pipes under considerable effect of thermogravitational forces*, in *Heat transfer and turbulent buoyant convection*, D.B. Spalding and N. Afgan, Editors. 1976, Hemisphere Publishing Corporation: Washington. p. 701-717.
[43] Jackson, T.W., W.B. Harrison, and W.C. Boteler, *Combined Free and forced convection in a constant temperature vertical tube.* Transactions ASME, 1958. **80**: p. 739-745.
[44] Brown, C.K. and W.H. Gauvin, *Combined free and forced convection: 1. Heat transfer in aiding flow.* The Canadian journal of Chemical Engineering., 1965. **1**: p. 306-312.
[45] Axcell, B.P. and W.B. Hall. *Mixed convection to air in a vertical pipe.* in *Proce. 6th Int. Heat Transfer Conference*. 1978. Toronto, Canada.
[46] Fewster, J. and J.D. Jackson. *Enhancement of turbulent heat transfer due to buoyancy for downward flow of water in vertical tubes.* in *Proc. Seminar on Turbulent Buoyant convection*. 1976. Beograd.
[47] Cebeci, T., A.A. Khattab, and R. LaMont. *Combined natural and forced convection in vertical ducts.* in *Proceddings of the Seventh International Heat transfer Conference.* 1982. Munchen, Fed. Rep. of Germany: Hemisphere Publishing Corporation.
[48] Osborne, D.G. and F.P. Incropera, *Laminar, mixed convection heat transfer for flow between horizontal parallel plates with asymmetric heating.* International Journal of Heat and Mass Transfer, 1985. **28**(1): p. 207-217.

[49] Jackson, J.D., M.A. Cotton, and B.P. Axcell, *Studies of mixed convection in vertical tubes.* International Journal of Heat and Fluid Flow, 1989. **10**: p. 2-15.
[50] Aicher, T. and H. Martin, *New correlations for mixed turbulent natural and forced convection heat transfer in vertical tubes.* International Journal of Heat Mass Transfer, 1997. **40**(15): p. 3617-3626.
[51] Sudo, Y., M. Kaminaga, and K. Minazoe, *Experimental study on the effects of channel gap size on mixed convection heat transfer characteristics in vertical rectangular channels heated from both sides.* Nuclear Engineering and Design, 1990. **120**(2-3): p. 135-146.
[52] Zhang, X. and S. Dutta, *Heat transfer analysis of buoyancy-assisted mixed convection with asymmetric heating conditions.* International Journal of Heat and Mass Transfer, 1998. **41**(21): p. 3255-3264.
[53] Dutta, S., X. Zhang, J.A. Khan, and D. Bell, *Adverse and favorable mixed convection heat transfer in a two-side heated square channel.* Experimental Thermal and Fluid Science, 1998. **18**(4): p. 314-322.
[54] ASHRAE, *ASHRAE Handbook Fundamentals*, ed. T. Circle. 2005, N.E., Atlanta.
[55] Churchill, S.W., *Friction-factor equation spans all fluid flow regimes.* Chemical engineering progress, 1977. **44**(81): p. 91-92.
[56] Winterton, R.H.S., *Where did the Dittus and Boelter equation come from?* International Journal of Heat and Mass Transfer, 1998. **41**(4-5): p. 809-810.
[57] White, F.M., *Viscous Fluid Flow*. Third Edition ed. 2006: McGraw-Hill International Edition.
[58] Kakac, S., *Transient turbulent flow in ducts.* Wärme- und Stoffübertragung, 1968. **1**: p. 169-176.
[59] Parametric Technology Corporation, *Mathcad 14*. 2007: Needham, MA.
[60] Hatton, A.P. and A. Quarmby, *The effect of axially varying and unsymmetrical boundary conditions on heat transfer with turbulent flow between parallel plates.* International Journal of Heat and Mass Transfer, 1963. **6**: p. 903-914.
[61] Kays, W., M. Crawford, and B. Weigand, *Convective heat and mass transfer*. 4th Edition ed. 2005: McGraw Hill. 546.
[62] Hallman, T.M., *Experimental study of combined forced and laminar convection in a vertical tube.* , in *TN D-1104*, NASA, Editor. 1961, Lewis Research Center: Cleveland, Ohio. p. 44.
[63] White, F.M., *Fluid Mechanics*. Fifth ed. Series in Mechanical Engineering. 2003: McGraw-Hill. 866.
[64] Barrow, H., *An analytical and experimental study of turbulent gas flow between two smooth parallel walls with unequal heat fluxes.* International Journal of heat and mass transfer, 1962. **5**: p. 469-487.